# Capacity Analysis for WDM Fiber-Radio Backbones With Star-Tree and Ring Architecture Incorporating Wavelength Interleaving

Christina Lim, *Member, IEEE*, Ampalavanapillai Nirmalathas, *Senior Member, IEEE*, Dalma Novak, *Senior Member, IEEE*, and Rodney Waterhouse, *Senior Member, IEEE*

***Abstract*—We present a model based on link budget calculations to investigate the capacity of a wavelength-division-multiplexed (WDM) fiber-radio backbone incorporating a wavelength-interleaving technique. The wavelength-interleaving technique improves the optical spectral efficiency of the millimeter-wave fiber-radio systems incorporating optical single sideband with carrier modulation. In this paper, we investigate the capacity limitations of WDM fiber-radio backbones incorporating both wavelength interleaving and optical single sideband with carrier modulation for star-tree and ring architecture. The analysis provides an estimation of the overall system capacity and an insight into the network layout and performance limitations.**

***Index Terms*—Architecture, fiber-radio access technology, fixed wireless access, millimeter-wave communications, network performance, optical fiber communications.**

## I. Introduction

HYBRID fiber-radio networks operating at millimeter-wave (mm-wave) frequencies (26–100 GHz) are being considered for the provision of future broadband interactive services [1]. In the typical architecture of a mm-wave wireless access system with optical fiber backhaul, the radio signals are generated at a central location before distribution via fiber to a number of remote antenna base stations (BSs) for wireless distribution [1]–[4]. Such an architecture moves the radio signal-processing and routing functions to the central office (CO), allowing the remote BSs to share resources, thereby simplifying the network architecture. The requirement for more BS due to the small coverage of mm-wave frequency radio signals demands the installation of functionally simple and compact BS. This can be achieved by implementing the RF-over-fiber transport scheme where the radio signal is distributed to and from the BS as a mm-wave modulated optical signal, which reduces the complexity of the electronics required at BSs, since frequency conversion hardware is not required there [5], [6]. However, the performance of RF-over-fiber transport scheme may be severely limited by fiber chromatic dispersion, which may degrade the received RF power of the mm-wave radio signals [7]–[9]. This effect can be overcome by using optical single sideband with carrier (OSSB+C) modulation [10]–[13]. Due to line-of-sight constraints of radio signals at mm-wave frequencies, a sectorized antenna interface is required at the antenna BS. Each sector may be fed by a different optical signal depending on the application. Such an approach is simplified by incorporating wavelength-division multiplexing (WDM) technology. WDM offers a number of advantages in terms of simplified upgrade and management of the radio network. However, implementing WDM in mm-wave fiber-radio systems with OSSB+C modulation leads to poor optical spectral efficiency since the typical WDM channel spacing is in excess of 50 GHz. Recently, we proposed and demonstrated a technique to increase the optical spectral efficiency in mm-wave WDM fiber radio via a wavelength-interleaving (WI) technique [14], [15]. In this scheme, the spectral efficiency of the optical network is greater than conventional WDM systems with standard wavelength channel spacings of 50 or 100 GHz.

In this paper, we further investigate our proposed wavelength-interleaving scheme to consider the network capacity and link budget requirements of a WDM mm-wave fiber-radio system incorporating both wavelength-interleaving technique and optical single sideband with carrier modulation. In doing so, we develop a network model based on link budget calculations to analyze the overall network capacity for fiber-radio backbone with both star-tree [16] and ring [17] architecture. Our analysis shows that an amplified optical link is essential for a total optical transmission distance of greater than 10 km for both architecture. If an amplified optical link is implemented, the placement of the optical amplifiers within the network is crucial to the overall network capacity and performance. There is a tradeoff between cost and network capacity for both architectures that needs to be considered.

This paper is organized as follows. Section II provides a description of the link budget model for investigating the network capacity limitations of a WDM mm-wave fiber-radio backbone. Section III describes the various scenarios where a star-tree architecture can be implemented and investigates the overall network capacity based on these scenarios while Section IV focuses on the capacity investigations of a four-node-ring network with similar scenarios as described in Section III. Finally, conclusions are presented in Section V.

Manuscript received January 30, 2003; revised July 24, 2003.

C. Lim and A. Nirmalathas are with the Australian Photonics Cooperative Research Centre, Photonics Research Laboratory, Department of Electrical and Electronic Engineering, The University of Melbourne, Melbourne, Australia (e-mail: c.lim@ee.mu.oz.au).

D. Novak and R. Waterhouse are with Corvis Subsea, Columbia, MD 21046 USA.

Digital Object Identifier 10.1109/JLT.2003.821763

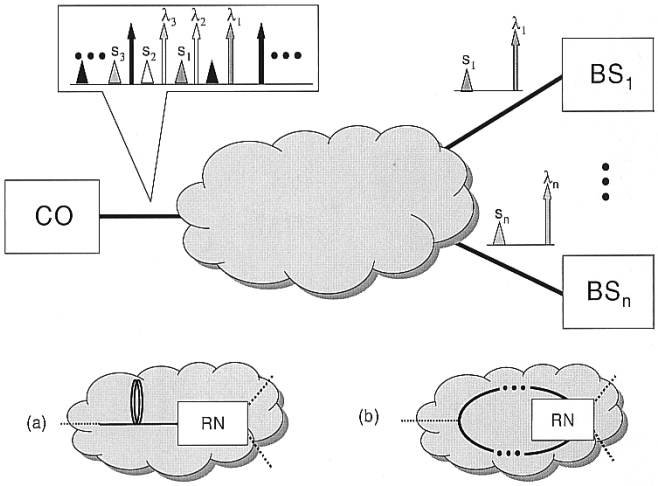


Fig. 1. Schematic diagram of WDM fiber-radio with (a) star-tree and (b) ring architecture.

## II. Network Model Based on Link Budget Calculations

Fig. 1 shows a schematic diagram of a WDM mm-wave fiber-radio system incorporating OSSB+C modulation and wavelength interleaving. The network can be deployed in a star-tree configuration as shown in Fig. 1(a) or in a ring configuration as shown in Fig. 1(b). At the CO, multiple WDM channels ($\lambda_1, \lambda_2 \ldots$) and the corresponding single sidebands ($s_1, s_2, \ldots$) are multiplexed together using a WI multiplexer (WI-MUX), and the modulated optical signals are transported to the remote node (RN) via an optical fiber network. At the RN, the WDM channels are demultiplexed using a WI demultiplexer (WI-DeMUX) before being routed to the designated BS. In the upstream path, multiple WDM channels are likewise received from the BSs before they are multiplexed at the RN via a WI-MUX and transported over the optical fiber network back to the CO.

In order to investigate the capacity of the fiber-radio network incorporating wavelength interleaving and OSSB+C modulation scheme, an ideal link budget model of the network was devised. Fig. 2 shows the schematic of the link budget model. The model assumes that each WDM channel is modulated by data in a binary phase-shift keyed format. The OSSB+C modulator is governed by the following transfer function:

$$E_{\text{out}}(t) = E_0 e^{j\omega_c t}\left(e^{j(\pi/2)(V_1(t)/V_\pi)} - e^{j(\pi/2)(V_1(t)/V_\pi)}\right) \quad (1)$$

where $E_{\text{out}}$ is the output optical field, $E_0 e^{j\omega t}$ represents the input optical field into the modulator, $\mathrm{V_1(t)}$ and $\mathrm{V_2(t)}$ are the electrical signal driving the two arms of the modulator, which can be represented by

$$V_1(t) = A\cos\left(\omega_m t + p(t) + V_b\right)$$
$$V_2(t) = A\sin\left(\omega_m t + p(t)\right) \quad (2)$$

where $A$ and $\omega_m$ are the amplitude and angular frequency of the modulating signal, $p(t)$ represents the data (0° or 180°), and $V_b$ is the modulator dc bias.

Neglecting higher order sidebands, the total average optical power for a single WDM channel can then be approximated using the optical carrier and the first-order sideband. These channels are multiplexed together at the CO and here optical crosstalk effects due to a nonideal optical WI-MUX or WI-DeMUX and the effects of fiber dispersion are not taken into account for the sake of simplicity. A black-box erbium-doped fiber amplifier (EDFA) [18] was used in the model to provide the optical amplification in the optical link. The saturated characteristics of the EDFA gain and the corresponding noise figure behavior with regards to input power are described by (3) and (4)

$$G = \frac{G_0}{1+\left(\frac{P_{\text{in}}}{P_{\text{sat}}}\right)^{\alpha}} = \frac{G_0}{1+\left(\frac{G_0 P_{\text{in}}}{P_{\max}}\right)^{\alpha}} \quad (3)$$

$$F = F_0 + k_1(\lambda)e^{k_2(\lambda)(G_0^{dB} - G^{dB})} \quad (4)$$

where $G_0$ and $G$ are the EDFA small-signal gain and the saturated gain for an input power of $P_{\text{in}}$ and $P_{\max}$ represents the maximum output power of the amplifier. $F_0$ and $F$ are the noise figures corresponding to the small-signal gain and the saturated gain in dB. $P_{\text{sat}}$, $\alpha$, $k_1$, and $k_2$ are unknown parameters that characterize the gain saturation and noise figure behavior that can be obtained via measured data of the EDFA.

The placement of the EDFA is dependent on the various scenarios that will be discussed in Section III. The WDM interleaved channels were transmitted over a fiber length of $L_{\text{SMF1}}$ before being demultiplexed at the RN, where the channels were then routed to the designated BS, which is located at a distance of $L_{\text{SMF2}}$ away. The gain and losses in the optical link are accumulated, and the bit error rate (BER) of a single channel received at the BS is then calculated based on the equivalent link gain or loss. Therefore, the entire fiber-radio backbone can be simplified to an equivalent link with an input of multiple noise-free WDM channels and equivalent noise contributions, as depicted in Fig. 2, where $G_{\text{equiv}}/L_{\text{equiv}}$ represents the equivalent gain/loss and $F_{\text{equiv}}$ represents the equivalent noise figure of the link. Table I shows the loss and gain values and also other parameters used in the model for the various components within the optical link, which are based on experimental data. In this model, the amplified spontaneous emission (ASE) noise resulting from the EDFA and thermal noise from the RF interface at the BS are taken into account. The noise characteristics of the network are assumed to be additive Gaussian noise and, therefore, the BER analysis is formulated in the Gaussian approximation for simplicity.

## III. Fiber-Radio Backbone Incorporating Star-Tree Architecture

Fig. 3(a)–(d) shows how a fiber-radio backbone with star-tree architecture can be deployed in a number of layouts. Here, the distance between the CO and RN is defined as the network reach length ($L_{\text{SMF1}}$) while the span between the RN and BS is defined as the spanout length of the network. Implementing the developed model and using parameter values obtained from actual typical optical component specifications, the various network layouts shown in Fig. 3(a)–(d) were investigated. Assuming a modulation frequency of 36 GHz for a single WDM channel and that an optical bandwidth of 30 nm is available via the EDFA gain bandwidth, a total of 52

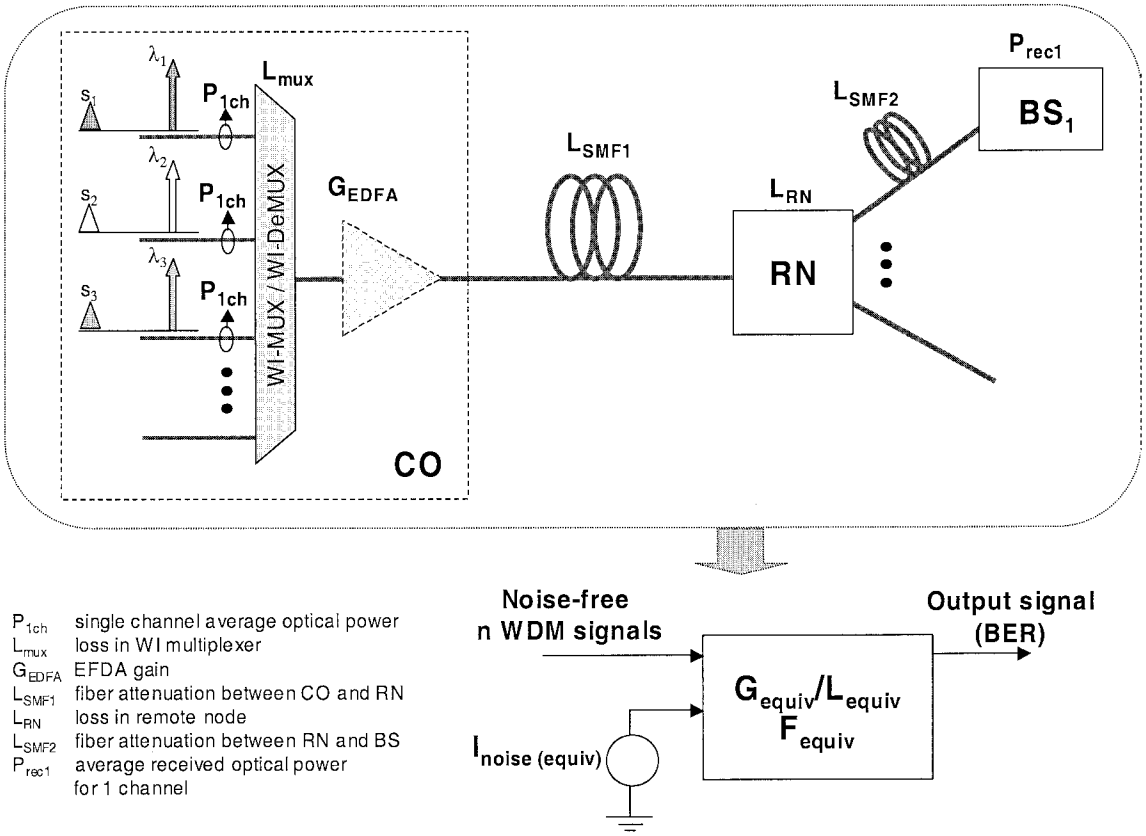


Fig. 2. Schematic diagram of fiber-radio backbone network model based on link budget calculation.

TABLE I
TABLE SHOWING THE LOSS/GAIN AND OTHER PARAMETERS USED IN THE ANALYTICAL MODEL FOR CAPACITY ANALYSIS BASED ON EXPERIMENTAL DATA

| | |
|---|---|
| Multiplexer loss ($L_{MUX}$) | 10 dB |
| Small-signal EDFA gain ($G_{EDFA}$) | 40 dB |
| EDFA maximum output power ($P_{MAX}$) | 18 dBm |
| OSSB+C modulator loss | 13 dB |
| Fiber attenuation | 0.2 dB/km |
| Remote node loss ($L_{RN}$) | 13 dB |
| Photodetector responsivity | 0.25 |
| Receiver sensitivity | -14 dBm |

WDM channels with OSSB+C modulation can be incorporated without wavelength interleaving for a set of wavelengths chosen by assuming a reference wavelength at 192.697 THz and a channel spacing of 72 GHz. If the WDM channels are interleaved, however, at a frequency spacing of 24 GHz, this capacity can be theoretically tripled to 156 channels. If the network has sufficient link budget, a passive optical network can be easily deployed as shown in Fig. 3(a). However, due to the limited link efficiency of transporting mm-wave modulated optical signals in a passive network, to achieve a maximum capacity of 156 wavelength-interleaved WDM channels for a spanout length of 1 km, the optical power input to the OSSB+C modulator per WDM channel ($P_{\mathrm{INC}}$) must be greater than $-3$ dBm, while the network reach length must be less than 9 km and the loss in the RN less than 6 dB.

For a more realistic and practical network layout, the network reach is assumed to be 50 km and the spanout length fixed at 5 km. Other optical device losses are assumed to be constant with

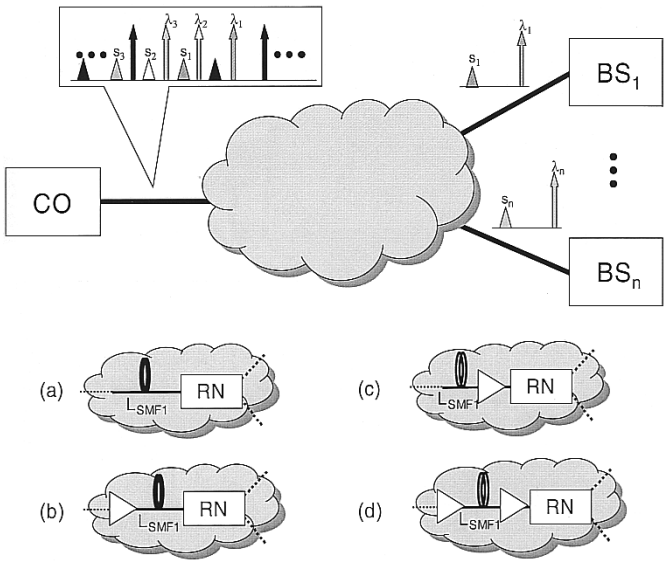


Fig. 3. Schematic diagram of WDM fiber-radio star-tree architecture with various network layout scenarios.

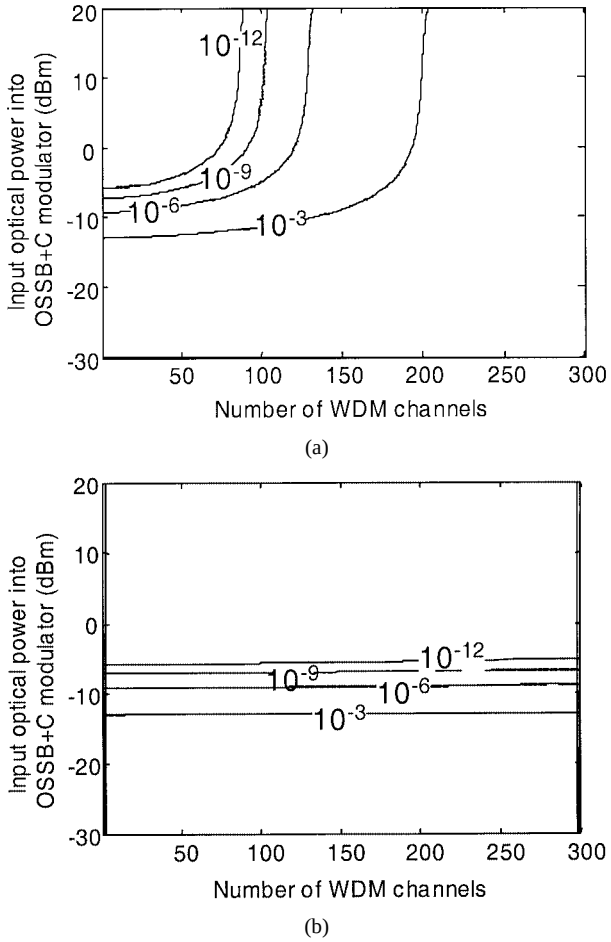


Fig. 4. BER contours for (a) preamplification and (b) postamplification layouts for star-tree configuration.

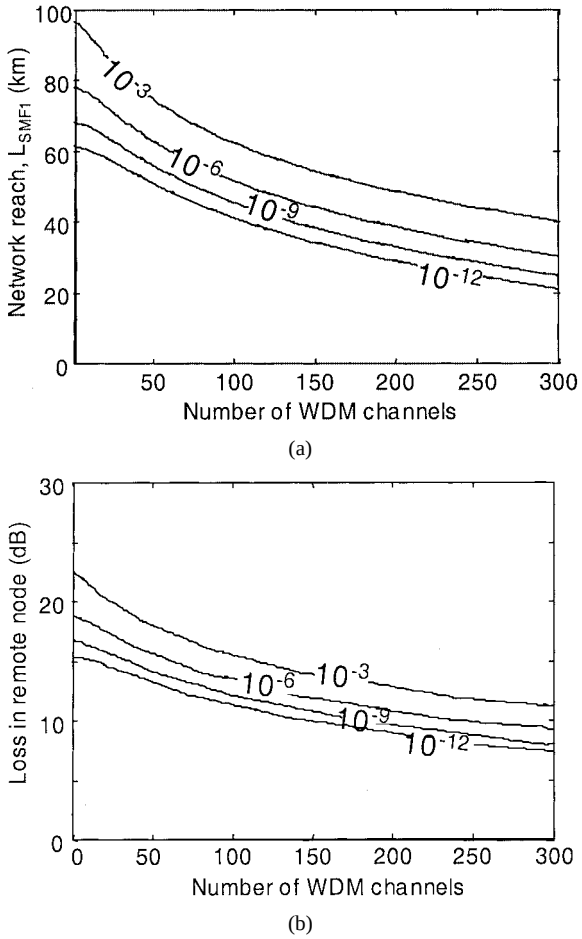


Fig. 5. BER contours for preamplification network layouts as a function of (a) network reach length ($L_{\mathrm{SMF1}}$) and (b) remote node loss for star-tree configuration.

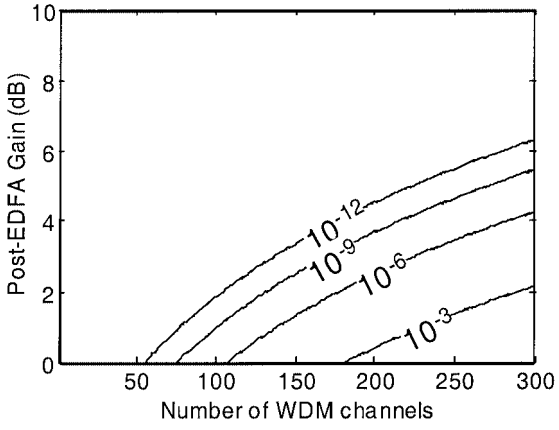


Fig. 6. BER contours for pre- and postamplification network layout for star-tree configuration.

values based on those measured in [5] with loss in the remote node set to 13 dB. The EDFA used in [5] has a small-signal gain of 40 dB and an output saturation power of 18 dBm. The most cost-effective placement of the optical amplifier is in the CO since network control and management is centralized and high-cost equipment can be shared among a large numbers of customer units (CUs), as depicted in Fig. 3(b). In order to analyze the network capacity limitation, the input optical power to the OSSB+C modulator per WDM channel ($P_{\mathrm{INC}}$) is varied as a function of the number of WDM channels, and the corresponding BER for a single received WDM channel at the BS is calculated. Fig. 4(a) shows the BER contours for a network layout with preamplification, i.e., the EDFA located at the CO as

TABLE II
SUMMARY OF THE NETWORK DIMENSIONS ACHIEVABLE FOR THE STAR-TREE ARCHITECTURE WITH DIFFERENT NETWORK TOPOLOGIES

| Network Topology | Reach Length (km) | Span-out Length (km) | Remote Node Loss (dB) | Comments |
|---|---|---|---|---|
| Passive | < 9 | 1 | < 6 | Limited by optical link efficiency |
| Pre-amplification | < 39 | 5 | 13 | Limited by EDFA saturations |
| Post amplification | 50 | 5 | 13 | Active remote node required |
| Pre- and post amplification | 50 | 5 | 13 | Needs > 2.5 dB gain at post amplifier |

depicted in Fig. 3(b). Due to EDFA saturation effects and signal quality degradation, the maximum capacity of 156 channels is reduced, as shown in Fig. 4(a). For example, assuming a typical $P_{\mathrm{INC}} = -3$ dBm and a BER$= 10^{-9}$, a total capacity of only 100 channels can be achieved with wavelength interleaving.

When the same EDFA is located at the RN [in the postamplification arrangement of Fig. 3(c)], the BER contours do not vary significantly with the number of WDM channels available in the system as depicted in Fig. 4(b). This indicates that the maximum total capacity of 156 channels can be achieved with this fiber-radio architecture. However, the implementation of an active RN will increase the overall system cost, maintenance, and management complexity. If the network reach length is allowed to vary while maintaining $P_{\mathrm{INC}} = -3$ dBm, $L_{\mathrm{SMF2}} = 5$ km, and remote node loss$= 13$ dB, it can be seen from Fig. 5(a) that to reach the maximum capacity (156 WDM channels) in the preamplification arrangement [Fig. 3(b)], $L_{\mathrm{SMF1}}$ (network reach length) must be less than 39 km. If the network reach length ($L_{\mathrm{SMF1}}$) and spanout length ($L_{\mathrm{SMF2}}$) were to be fixed at 50 and 5 km, respectively, and $P_{\mathrm{INC}} = -3$ dBm, while varying the remote node loss, it is shown in Fig. 5(b) that the maximum capacity can only be achieved for the preamplification arrangement under the specified conditions if the remote node loss is less than 11 dB. Therefore, maximum capacity of 156 WDM channels can only be reached for the preamplification configuration for $P_{\mathrm{INC}} = -3$ dBm and $L_{\mathrm{SMF2}} = 5$ km, is either by reducing $L_{\mathrm{SMF1}}$ to less than 39 km or reducing remote node loss to less than 11 dB.

An alternative network layout scenario as shown in Fig. 3(d) utilizes both pre- and postamplification in the CO and the RN, respectively. In such an architecture, most of the overall link gain is located at the preamplifier while the postamplifier aims to provide sufficient gain. Maintaining a network reach length of 50 km, spanout length of 5 km, remote node loss of 13 dB, and $P_{\mathrm{INC}} = -3$ dBm while varying the postamplifier gain and the number of WDM channels, Fig. 6 presents the calculated received BER contours at the BS for a single WDM channel. To achieve the maximum system capacity of 156 channels while maintaining the received signal BER at $10^{-9}$, an additional minimum gain of 2.5 dB is required at the postamplifier. These results clearly show that if cost can be compromised, a small gain block located at the RN to overcome additional losses within the RN and BS will increase not only the network reach length but also the overall system capacity. Table II summarizes the dimensions of the network considered for the various topologies for the star-tree architecture.

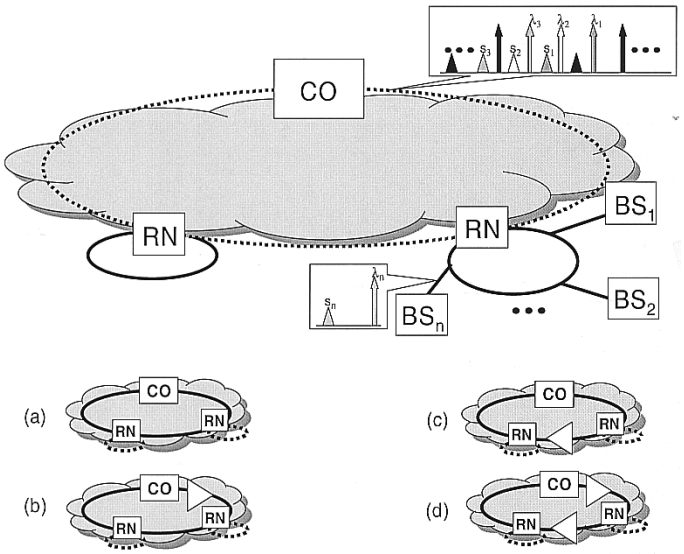


Fig. 7. Schematic diagram of WDM fiber-radio ring architecture with various network layout scenarios.

## IV. FIBER-RADIO BACKBONE INCORPORATING RING ARCHITECTURE

Fig. 7 shows a schematic diagram of a WDM fiber-radio backbone with a primary ring architecture incorporating WI and OSSB+C modulation. The primary ring interconnects the central office to a number of remote nodes. The RNs are then connected to a secondary ring network that links all the antenna BSs. At the CO, multiple WDM channels are multiplexed together and distributed to the RNs via the optical ring network. At each RN, a block containing a number of WDM channels is dropped before each of the WDM channels is routed to the designated BS via the secondary ring. In the upstream path, the WDM channel at the same wavelength as the dropped channel is added back into the network before being routed back to the CO.

In the analysis used here, the rings are unidirectional, the secondary ring network is assumed to be completely passive, the RNs are equally spaced within the primary ring, and the BSs are equally spaced within the secondary ring. Similarly, in the

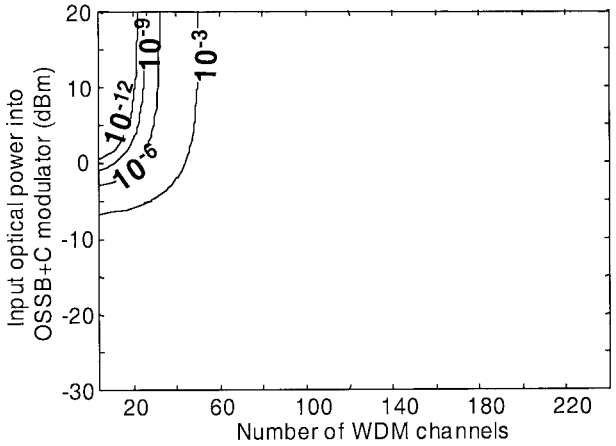


(a)

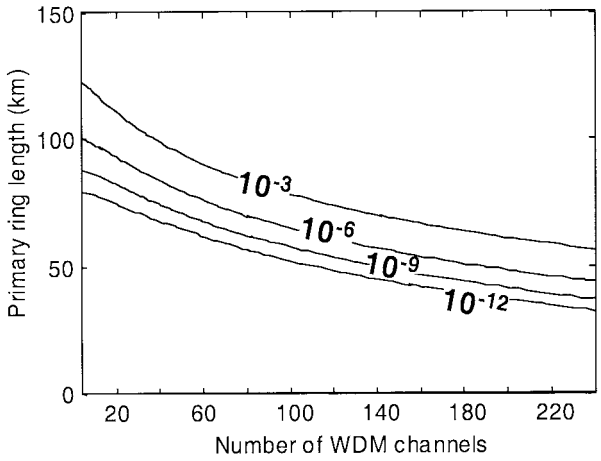


(b)

Fig. 8. BER contours for preamplification network layouts as a function of (a) input optical power into OSSB+C modulator ($P_{\mathrm{INC}}$) and (b) primary ring length for a four-node-ring architecture.

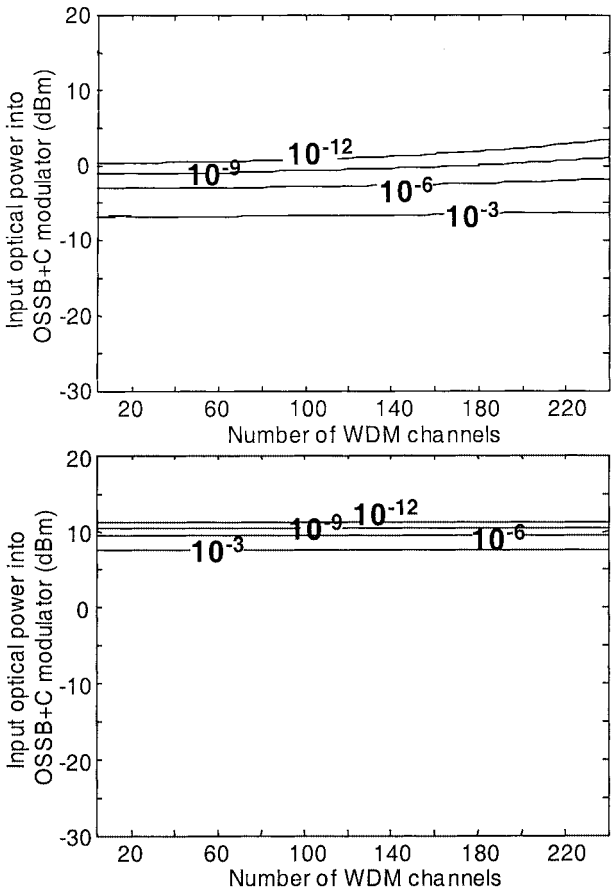


Fig. 9. BER contours for midspan amplification network layout for (a) RN4 and (b) RN2 for a four-node-ring architecture.

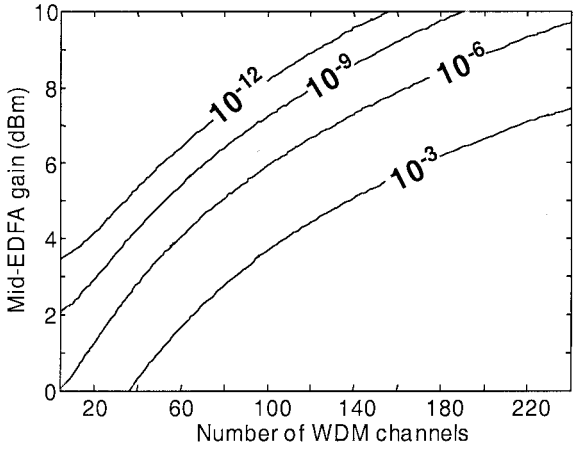


Fig. 10. BER contours for pre- and midway amplification network layouts for four-node-ring architecture.

deployment of the network, the primary ring can be deployed in a number of layouts as highlighted in Fig. 7 and as previously discussed in Section III. The various network layouts shown in Fig. 7 incorporating four RNs were investigated using the link budget model. As before, assuming a modulation frequency of 36 GHz, the EDFA gain bandwidth of 30 nm, and that the channels are interleaved at a frequency spacing of 24 GHz with a reference optical wavelength of 192.697 THz, the analysis shows that to achieve a maximum capacity of 156 wavelength-interleaved channels for a completely passive network [Fig. 7(a)], the input optical power to the OSSB+C modulator per single WDM channel ($P_{\mathrm{INC}}$) must be greater than $-3$ dBm for a secondary ring length of 2 km, while the primary ring length must be less than 10 km, with the loss in RN$<\sim 1$ dB.

For a more practical network layout, the primary ring length is assumed to be 100 km and secondary ring length fixed to 10 km. Again the parameters used for the EDFA, remote node loss, and other optical devices in this model were the same as those used in the star-tree architecture. Similarly, to analyze the network capacity and performance $P_{\mathrm{INC}}$ is varied as a function of the total number of WDM channels and the corresponding BER for a single received WDM channel at the BS located midspan within the secondary ring. The analysis was carried out for a BS in each RN. Shown in Fig. 8(a) are the BER contours for the WDM channel received at the last RN (RN4) with preamplification [an EDFA located in the CO as in Fig. 7(b)] in the network layout. Only the BER contours of the last RN are shown as the received signals will be the weakest and most susceptible to noise. For $P_{\mathrm{INC}} = 0$ dBm and a BER$= 10^{-9}$, the maximum capacity reduces from 156 to approximately 13 channels, which can be attributed to EDFA saturation effects and signal quality degradation. If the primary ring length is allowed to vary while

TABLE III
SUMMARY OF THE NETWORK DIMENSIONS ACHIEVABLE FOR THE RING ARCHITECTURE WITH DIFFERENT NETWORK TOPOLOGIES

| Network Topology | Primary Ring Length (km) | Secondary Ring Length (km) | Remote Node Loss (dB) | Comments |
|---|---|---|---|---|
| Passive | < 10 | 2 | < 1 | Limited by optical link efficiency |
| Pre-amplification | < 50 | 10 | 13 | Limited by EDFA saturations |
| Mid-way amplification | 100 | 10 | 13 | Remote Node 2 (RN2) base station requires an input optical power of +11 dBm – not practical |
| Pre- and mid-way amplification | 100 | 10 | 13 | Needs > 9 dB gain at mid-way amplifier |

maintaining $P_{\mathrm{INC}} = 0$ dBm and secondary ring length of 10 km, it can be seen from Fig. 8(b) that to achieve maximum capacity of 156 WDM channels, the primary ring length is limited to less than 50 km. When the same EDFA is located midspan through the primary ring (between RN2 and RN3), as shown in Fig. 7(c), the BER contours at RN4 indicate that for $P_{\mathrm{INC}} = 0$ dBm, a maximum capacity of 156 channels is achievable as depicted in Fig. 9(a). However, the BER contours received at RN2 (before optical amplification) as shown in Fig. 9(b) indicate that the network requires a $P_{\mathrm{INC}}$ of at least $+11$ dBm to achieve a BER$= 10^{-9}$ independent of the total network capacity, which is not achievable practically.

An alternative network layout scenario for the primary ring, as shown in Fig. 7(d), incorporates the both pre- and midspan amplification where most of the overall link gain is located at the preamplifier in the CO while the midspan amplifier aims to overcome additional losses within the ring. Maintaining the primary ring length of 100 km and the secondary ring length at 10 km and an input power $P_{\mathrm{INC}} = 0$ dBm while varying the midspan amplifier gain and the number of WDM channels, Fig. 10 represents the BER contours at the BS located at the last RN (RN4) for a single WDM channel. To achieve the maximum system capacity of 156 channels while maintaining the received signal at BER$= 10^{-9}$, a minimum gain block of at least 9 dB is required midway through the primary ring. These simulations clearly indicate that to maintain a fiber-radio backbone incorporating a primary ring network of 100 km and a secondary passive ring of 10 km, cost has to be compromised as a small and sufficient gain block is required within the primary ring in addition to the preamplification located in the CO to overcome losses and also increases the overall system capacity. Table III summarizes the network dimensions achievable for the various network topologies for the ring architecture.

## V. CONCLUSION

We have investigated network capacity limitations for a star-tree and a four-node-ring WDM mm-wave fiber-radio systems incorporating wavelength-interleaving technique to increase optical spectral efficiency. A model was developed based on link budget calculations to provide estimations of the network capacity, which can also be utilized to find the optimum network architecture in conjunction with other factors such as cost. It was found that a completely passive feeder network offers simplicity; however, it is limited by a maximum network reach of 9 km for the star-tree configuration and a maximum primary ring length of 9 km for the ring architecture. Although a preamplification arrangement is the most cost-effective configuration and also enables a centralized control architecture, amplifier saturation effects limit the overall system capacity to 100 channels with a network reach of 50 km for star-tree architecture. The effect is more pronounced for ring network, where the total capacity is limited to fewer than 15 WDM channels for primary and secondary ring lengths of 100 and 10 km, respectively. Incorporating an amplified RN architecture (postamplification) significantly increases the overall capacity for the star-tree network; and likewise, incorporating a small amplifier block midway within the primary ring of a ring network significantly increases the overall capacity. However, such an amplification arrangement is accompanied by an increased cost and network management complexity tradeoffs, which must also be taken into account.

## REFERENCES

[1] R. Heidemann and G. Veith, "MM-wave photonics technologies for Gbit/s-wireless-local-loop," in *Proc. OECC*, Chiba, Japan, 1998.
[2] D. Novak, G. H. Smith, C. Lim, A. Nirmalathas, H. F. Liu, and R. B. Waterhouse, "Fiber-fed millimeter-wave wireless systems," in *Proc. OECC'98*, Chiba, Japan, 1998, pp. 306–307.
[3] U. Gliese, "Multi-functional fiber-optic microwave links," *Opt. & Quantum Electron.*, vol. 30, pp. 1005–1019, 1998.
[4] H. Ogawa, D. Polifko, and S. Banba, "Millimeter-wave fiber optics systems for personal radio communications," *IEEE Trans. Microwave Theory Tech.*, vol. 40, pp. 2285–2292, 1992.
[5] G. H. Smith, D. Novak, and C. Lim, "A millimeter-wave full-duplex fiber-radio star-tree architecture incorporating WDM and SCM," *IEEE Photon. Technol. Lett.*, vol. 10, pp. 1650–1652, 1998.
[6] L. Noel, D. Wake, D. G. Moodie, D. D. Marcenac, L. D. Westbrook, and D. Nesset, "Novel techniques for high-capacity 60 GHz fiber-radio transmission systems," *IEEE Trans. Microwave Theory Tech.*, vol. 45, pp. 1416–1423, 1997.
[7] G. J. Meslener, "Chromatic dispersion induced distortion of modulated monochromatic light employing direct detection," *IEEE J. Quantum Electron.*, vol. QE-20, no. 10, pp. 1208–1216, 1984.

[8] H. Schmuck, "Comparison of optical millimeter-wave system concepts with regard to chromatic dispersion," *Electron. Lett.*, vol. 31, pp. 1848–1849, 1995.
[9] U. Gliese, S. Norskov, and T. N. Nielsen, "Chromatic dispersion in fiber-optic microwave and millimeter-wave links," *IEEE Trans. Microwave Theory Tech.*, vol. 44, no. 10, pp. 1716–1724, 1996.
[10] G. H. Smith, D. Novak, and Z. Ahmed, "Technique for optical SSB generation to overcome dispersion penalties in fiber-radio systems," *Electron. Lett.*, vol. 33, no. 1, pp. 74–75, 1997.
[11] J. Park, W. V. Sorin, and K. Y. Lau, "Elimination of the fiber chromatic dispersion penalty on 1550 nm millimeter-wave optical transmission," *Electron. Lett.*, vol. 33, no. 6, pp. 512–513, 1997.
[12] E. Vergnol, D. Tanguy, J. F. Cadiou, A. Carenco, and E. Penard, "Multi-carrier and m-QAM modulation based on integrated single side band lightwave source," in *Proc. OFC'99*, San Diego, CA, 1999, TuP3–1.
[13] E. Vourch, D. Le Berre, and D. Herve, "Lightwave single sideband source using a wavelength self-tunable inp:fe filter for fiber-wireless systems," in *Proc. MWP2001*, Long Beach, CA, USA, 2002, pp. 199–202.
[14] C. Lim, A. Nirmalathas, D. Novak, R. S. Tucker, and R. B. Waterhouse, "Technique for increasing optical spectral efficiency in millimeter-wave WDM fiber-radio," *Electron. Lett.*, vol. 37, no. 16, pp. 1043–1045, 2001.
[15] H. Toda, T. Yamashita, K. Kitayama, and T. Kuri, "A DWDM MM-wave fiber-radio system by optical frequency interleaving for high spectral efficiency," in *Proc. MWP2001*, Long Beach, CA, 2002, pp. 85–88.
[16] C. Lim, A. Nirmalathas, D. Novak, and R. B. Waterhouse, "Capacity analysis for a WDM fiber-radio backbone incorporating wavelength-interleaving," in *Proc. OFC*, Anaheim, CA, 2002, pp. 355–357.
[17] ——, "Network performance and capacity analysis for a ring WDM fiber-radio backbone incorporating wavelength-interleaving," in *Proc. OECC*, Yokohama, Japan, July 2002, pp. 194–195.
[18] X. Zhang and A. Mitchell, "A simple black box model for erbium-doped fiber amplifiers," *IEEE Photon. Technol. Lett.*, vol. 12, pp. 28–30, 2000.

**Christina Lim** (S'98–M'00) received the B.E. (with first-class honors) and the Ph.D. degrees in electrical and electronic engineering from the University of Melbourne, Melbourne, Australia, in 1995 and 2000, respectively.

She was one of the recipients of the IEEE Lasers & Electro-Optics Society (LEOS) Graduate Student Fellowship in 1999. In 1999, she joined the Photonics Research Laboratory (PRL), a member of the Australian Photonics Cooperative Research Centre (APCRC), at the University of Melbourne, where she is now a Senior Research Fellow. Her research interests include fiber-wireless access technology, modeling of optical and wireless communication systems, microwave photonics, application of mode-locked lasers, optical network architectures, and optical signal monitoring.

**Ampalavanapillai Nirmalathas** (M'98–SM'03) received the degrees of B.E. (Hons.) and Ph.D. degrees in electrical and electronic engineering from the University of Melbourne, Melbourne, Australia, in 1993 and 1997, respectively.

In 1997, he joined the Photonics Research Laboratory (PRL), a member of the Australian Photonics Cooperative Research Centre (APCRC), at the University of Melbourne, where he held Research Fellow and Senior Research Fellow positions before moving to his current position as a Senior Lecturer. He is also the Director of PRL and the Program Manager of the Telecommunications Technologies Research Program in the APCRC. His current research interests include fibre-wireless networks, optical networks, optical signal monitoring, photonic packet switching technologies, ultrafast optical communications systems, and applications of mode-locked semiconductor lasers.

Dr. Nirmalathas is also the IEEE Lasers & Electro-Optics Society (LEOS) representative on the Steering Committee of the CLEO Pacific Rim Conference and he has been a Member of committees associated with a number of international conferences in his field of expertise.

**Dalma Novak** (S'90–M'91–SM'02) received the B.E. (with first-class honors) and Ph.D. degrees in electrical engineering from the University of Queensland, Brisbane, Australia, in 1987 and 1992, respectively. Her doctoral thesis investigated the dynamic behavior of directly modulated semiconductor lasers.

From January 1992 to August 1992, she was a Lecturer in the Department of Electrical and Computer Engineering at the University of Queensland. In September 1992, she joined the Photonics Research Laboratory (PRL), a member of the Australian Photonics Cooperative Research Centre (APCRC), in the Department of Electrical and Electronic Engineering at the University of Melbourne, Melbourne, Australia, where her responsibilities over the years have included Deputy Director and Research Director of PRL, CRC Key Researcher, Director of the CRC Melbourne Division, and CRC Education Director and where she also currently holds the positions of Associate Professor and Reader. From December 1999 to March 2001, she was a Director of Australian Photonics Pty, Ltd. From July 2000 to January 2001, she was a Visiting Researcher in the Department of Electrical Engineering, University of California Los Angeles (UCLA), and the Naval Research Laboratory, Washington, DC, respectively. In June 2001, she joined Dorsál Networks, Inc., now part of Corvis Corporation, Columbia, MD, where she is a Technical Section Lead. Her research interests include fiber-radio communication systems and high-speed optoelectronic devices and circuits. She has authored or coauthored more than 160 papers in these areas.

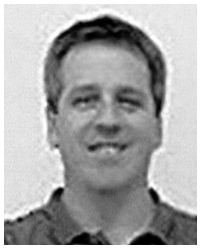

**Rodney Waterhouse** (S'90–M'92–SM'02) received the B.E. (Hons.), M.Eng.Sc. (Research), and Ph.D. degrees from the University of Queensland, Brisbane, Australia, in 1987, 1990, and 1994, respectively.

In 1994, he joined the School of Electrical and Computer Engineering at the RMIT University as a Lecturer and became a Senior Lecturer in 1997. From mid-2000 to the beginning of 2001, he was a Visiting Professor at the Department of Electrical and Computer Engineering, University of California, Los Angeles (UCLA) for three months and then a Visiting Researcher in the Photonics Technology Branch of the Naval Research Laboratories, Washington, DC, for three months while on sabbatical. In June 2001, he took a leave of absence from RMIT and joined Dorsal Networks, now part of Corvis Corporation, based in Columbia, MD. His research interests include optically distributed wireless systems, photonic devices, optical systems, and wireless communication technologies. He has published more than 150 papers and has three patents in these areas.